

Article

¹⁵N Stable Isotope Labeling PSTs in *Alexandrium minutum* for Application of PSTs as Biomarker

Wancui Xie ^{1,2}, Min Li ¹, Lin Song ^{1,2}, Rui Zhang ³, Xiaoqun Hu ¹, Chengzhu Liang ⁴ and Xihong Yang ^{1,2,*}

¹ College of Marine Science and Biological Engineering, Qingdao University of Science & Technology, Qingdao 266042, China; xiewancui@163.com (W.X.); 2017170007@mails.qust.edu.cn (M.L.); lybinsong@hotmail.com (L.S.); 2018170002@mails.qust.edu.cn (X.H.)

² Key Laboratory for Biochemical Engineering of Shandong Province, Qingdao 266042, China

³ College of Food Science and Technology, Guangdong Ocean University, Zhanjiang 524088, China; zhangr1168@163.com

⁴ Shandong Entry-Exit Inspection and Quarantine Bureau, Qingdao 266000, China; liangcz@163.com

* Correspondence: 03137@qust.edu.cn

Received: 27 February 2019; Accepted: 4 April 2019; Published: 8 April 2019



Abstract: The dinoflagellate *Alexandrium minutum* (*A. minutum*) which can produce paralytic shellfish toxins (PSTs) is often used as a model to study the migration, biotransformation, accumulation, and removal of PSTs. However, the mechanism is still unclear. To provide a new tool for related studies, we tried to label PSTs metabolically with ¹⁵N stable isotope to obtain ¹⁵N-PSTs instead of original ¹⁴N, which could be treated as biomarker on PSTs metabolism. We then cultured the *A. minutum* AGY-H46 which produces toxins GTX1-4 in f/2 medium of different ¹⁵N/P concentrations. The ¹⁵N-PSTs' toxicity and toxin profile were detected. Meanwhile, the ¹⁵N labeling abundance and ¹⁵N atom number of ¹⁵N-PSTs were identified. The ¹⁴N of PSTs produced by *A. minutum* can be successfully replaced by ¹⁵N, and the f/2 medium of standard ¹⁵N/P concentration was the best choice in terms of the species' growth, PST profile, ¹⁵N labeling result and experiment cost. After many (>15) generations, the ¹⁵N abundance in PSTs extract reached 82.36%, and the ¹⁵N atom number introduced into GTX1-4 might be 4–6. This paper innovatively provided the initial evidence that ¹⁵N isotope application of labeling PSTs in *A. minutum* is feasible. The ¹⁵N-PSTs as biomarker can be applied and provide further information on PSTs metabolism.

Keywords: *Alexandrium minutum*; dinoflagellate; paralytic shellfish toxins (PSTs); ¹⁵N stable isotope labeling; biomarker

Key Contribution: The ¹⁴N of paralytic shellfish toxins produced by experimental *Alexandrium minutum* can be replaced by ¹⁵N successfully. ¹⁵N abundance in paralytic shellfish toxins extract reached 82.36%, and ¹⁵N atom number introduced into Gonyautoxin1-4 may be 4–6. ¹⁵N-paralytic shellfish toxins as biomarker have potential application in some fields such as metabolomics and clinical mechanism of paralytic shellfish toxins.

1. Introduction

Harmful algal blooms (HABs) occur frequently in coastal areas worldwide, causing public concerns. Firstly, HABs cause millions of dollars economic losses in the tourism and industry sectors [1]. Secondly, HABs break the balance of marine ecosystems as they can disrupt communities and food web structures [2,3]. Thirdly, phycotoxins produced by HABs may be transferred through the food cycle, thereby causing lethal and sublethal effects on humans [4,5]. Among all the toxins produced by HABs

species, paralytic shellfish toxins (PSTs) produced by dinoflagellates are the most widespread and potent shellfish contaminating biotoxins [6]. They are accumulated by filter-feeding bivalve mollusks and some zoophagous mollusks [7]. One of the most widespread toxigenic microalgal taxa is the dinoflagellate *Alexandrium*, and studies have demonstrated that toxic *Alexandrium* spp. disrupt behavioral and physiological processes in marine filter feeders [8,9]. In recent years, *A. tamarense*, *A. minutum*, *A. ostenfeldii*, and others were used as carriers of PSTs to track the migration, biotransformation, accumulation, and removal of PSTs under experimental conditions [10–12]. However, the metabolism of PSTs in bivalves is still unclear. Thus, there is a need for a new powerful tool to conduct PST-related researches.

Isotopic tracer technique can be used to study the absorption, distribution, metabolism, and excretion of some substances, such as protein and lipid, or to establish organism trophic links in the ecosystem [13–16]. The stable isotope labeling (ICAT, ICPL, IDBEST, iTRAQ, TMT, IPTL, and SILAC)-based quantitative approaches are highly efficient for obtaining highly accurate quantification results and for building more extensive small molecule databases [14,17], especially in proteomics [18,19]. Some studies were conducted on microalgae due to their ability to fix stable isotopes photosynthetically into cells and offer various target products [20–23]. Artificially enriched stable isotopes of nitrogen can be fed to cells, either in the form of ^{15}N -labeled amino acid or ^{15}N -labeled inorganic salt. According to [24], the microalgae *Chlamydomonas reinhardtii* was used to produce ^{15}N -labeled amino acids with a high isotopic enrichment and sixteen ^{15}N -labelled amino acids could be obtained.

However, isotope-labeling toxin-producing algae have been rarely studied so far. In the present study, we metabolically labeled the *A. minutum* produced gonyautoxins1-4 (GTX1-4) that belonging to mono-sulfated subgroup of PSTs [25]. The culture was carried out with ^{15}N - NaNO_3 as nitrogen source to obtain the ^{15}N -PSTs that could be used as biomarker and provide further information on PSTs metabolism in filter feeding bivalve.

2. Results

2.1. Batch Culture: $^{15}\text{N}/\text{P}$ Influence in Algal Growth and Toxicity

Initial batch culture experiments allowed comparison of algae growth under different $^{15}\text{N}/\text{P}$ conditions, as follows: Group A: 1.0 time of the f/2 medium standard $^{15}\text{N}/\text{P}$ concentration; Group B: 1.5 times of the f/2 medium standard $^{15}\text{N}/\text{P}$ concentration; Group C: 2.0 times of the f/2 medium standard $^{15}\text{N}/\text{P}$ concentration; Group D: 2.5 times of the f/2 medium standard $^{15}\text{N}/\text{P}$ concentration; and Group E: 3.0 times of the f/2 medium standard $^{15}\text{N}/\text{P}$ concentration. The results showed that $^{15}\text{N}/\text{P}$ concentration can affect algal growth (Figure 1a). In an optimal culture environment, the growth curve of algae cell can be roughly divided into 4 phases, as follows: lag phase 0–15 days; log phase 16–30 days; 31 days of the stable phase; and decay phase. In this study, the decay phase was not studied, because the focus was on the degree of ^{15}N labeling of algal cellular toxin. The results were similar to those obtained in the report [26]. However, the lag phase of this experiment was much longer, and it may have been caused by partial mechanical damage to cells when algal cells were collected by centrifugation. After the growth of algal cells into the log phase, Group B cell density was higher than those of the other four groups ($p < 0.05$). At 30 days, the maximum value of Group B reached 3.820×10^4 cells/mL, and there was no significant difference in Group A cell density (3.342×10^4 cells/mL) ($p > 0.05$). However, the biomass of Groups A and B biomass was much higher than that of the other three groups ($p < 0.01$). Lower biomass at high nutrient concentration could be attributed to the inhabitation of photosystem II's photosynthetic capacity at high nutrient levels [27].

$^{15}\text{N}/\text{P}$ conditions also can affect toxicity of algae cells (Figure 1b). The highest toxin levels were determined at day 25 in the log phase in all groups, the same as [28], not early- or post- stationary growth phase mentioned in [29,30]. Concerning the factors influencing toxicity, the toxin content per cell in batch culture was not only related to the cell growth stage, but was also affected by intracellular

medium standard ¹⁵N/P and ¹⁴N/P concentration, indicating that the application of ¹⁵N isotope labeling can feasibly be used to study PSTs production and metabolism.

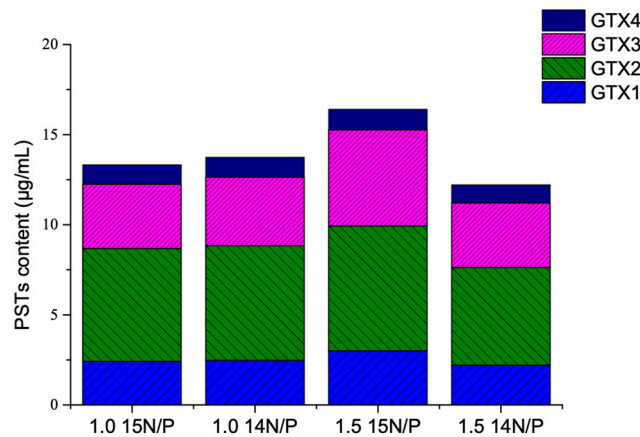


Figure 3. The effects of ¹⁵N/P concentration on *A. minutum* PST profile.

2.4. ¹⁵N Labeling Abundance Change of ¹⁵N-PSTs

The ¹⁵N labeling abundance was calculated according to the following formula:

$$\begin{aligned}
 {}^{15}\text{N atom\%} &= 1/(2I_{28}/I_{29} + 1) \times 100 \quad ({}^{15}\text{N atom\%} < 10\%); \\
 {}^{15}\text{N atom\%} &= 2/(I_{29}/I_{30} + 2) \times 100 \quad ({}^{15}\text{N atom\%} > 10\%)
 \end{aligned}
 \tag{1}$$

In the algal culture environment, ¹⁵N-NaNO₃ of f/2 medium is not the only nitrogen source because of the inorganic ¹⁴N existing in natural seawater. *A. minutum* cells prefer absorbing light elements (¹⁴N) and rejecting heavy elements (¹⁵N), resulting in nitrogen stable isotope fractionation. With increasing cell density and size, less and less ¹⁴N can be utilized. Thus, more ¹⁵N can enter cells, and nitrogen stable isotopes fractionation weakens. Two culture methods and gas isotope mass spectrometer were used to determine the relationship between ¹⁵N-labeling abundance and culture time, as shown in Table 1. During the batch culture, ¹⁵N abundance was positively related to culture time and reached the highest value at day 30. There are significant differences (*p* < 0.01) in terms of ¹⁵N abundance among lag, log, and stable phases. After many generations, ¹⁵N abundance reached to 82.36 atom%, but this percentage was still far below the abundance of the labeling material ¹⁵N-NaNO₃ (δ¹⁵N = 99.14%), not reaching our expectation (>90%).

Table 1. ¹⁵N labeling abundance change of PSTs along with the change of culture time in different cultivation methods.

Culture Method		1.0 Time of the f/2 Medium Standard	1.5 Times of the f/2 Medium Standard
		¹⁵ N/P Concentration	¹⁵ N/P Concentration
PSTs ¹⁵ N Abundance (Atom%)			
Batch culture/d	0	0.47	0.47
	20	26.26	26.43
	30	57.16	70.26
Generation to generation culture/generation	1	37.60	-
	2	58.32	-
	3	62.46	-
No. n generation	-	82.36	-

2.5. The Efficiency of ^{15}N -PSTs Separation and Purification

^{15}N -PSTs extracts were separated and purified by column chromatography on the Bio-Gel P-2 and the weak cation exchanger Bio-Rex 70. In the process of column chromatography on the Bio-Gel P-2, fluorescence detection and UV absorbance detection were carried out (Figure 4a). The UV absorption peak did not coincide with the fluorescence absorption peak. Thus, the UV absorption signal had no relationship with the toxin component. As shown by the fluorescence absorption peak, Bio-Gel P-2 effectively separated ^{15}N -PSTs with impurities in crude extracts, such as proteins and pigments. The liquid of fluorescence absorption peak was collected, freeze-dried (10 mg), and redissolved with 0.05 M Tri-HCl (2 mL). The redissolved sample (1 mL) was used for purification by column chromatography on weak cation exchanger Bio-Rex 70 at gradient elution condition and was separated (Figure 4b). After analysis, the Peak I was determined to be the isomer mixture of GTX1/4, and Peak II was the isomer mixture of GTX2/3.

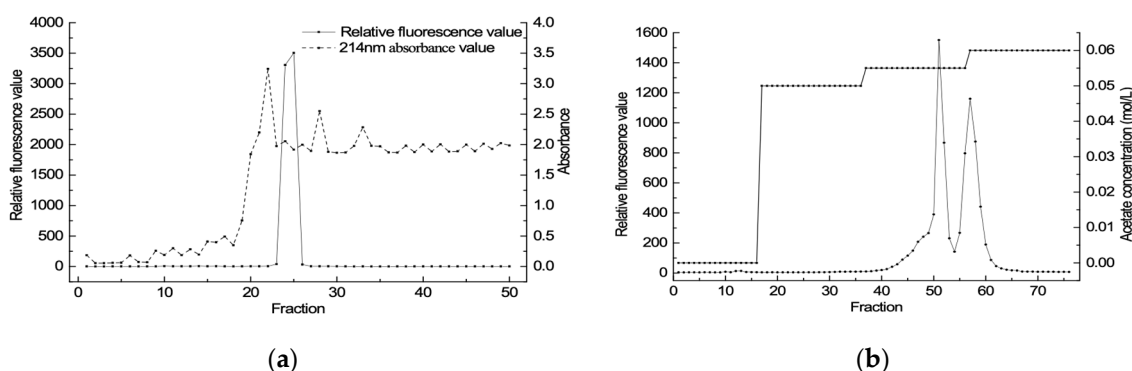


Figure 4. Gonyautoxin1-4 purified by column chromatography on the Bio-Gel P-2 (a) and the weak cation exchanger BioRex 70 (b).

2.6. ^{15}N Atom Number Identification of ^{15}N -PSTs

As demonstrated previously [32], GTX1-4 (Figure 5) can be ionized in ESI positive ion mode, thereby giving abundant fragment ions (Table 2). When ^{14}N of PSTs is replaced by ^{15}N , $[\text{M}+\text{H}]^+$ and fragment ions will change with the number of ^{15}N atoms, so that primary mass spectrum can be used to determine the ^{15}N atom number of ^{15}N -PSTs. After the addition of artificial nitrogen in *A. minutum* culture, ^{15}N was successfully introduced to PSTs, and characteristic fragment ions were produced. There was no $[\text{M}+\text{H}]^+$ peak in the mass spectrum as the result of high capillary voltage in this experiment (Figure 6). GTX1 produced three characteristic fragment ions ($m/z = 334.2966$; 318.3007 ; 319.3054) with the loss of $-\text{SO}_3$ or $-\text{SO}_3-\text{H}_2\text{O}$. GTX4 generated three characteristic fragment ions ($m/z = 318.3007$; 319.3054 ; 338.3418) with the loss of $-\text{SO}_3-\text{H}_2\text{O}$ or $-\text{SO}_3$ and had two fragment ions ($m/z = 318.3007$; 319.3054) similar to those of GTX1. There were four characteristic fragment ions ($m/z = 322.1197$; 321.1252 ; 305.1583 ; 317.0497) in GTX2 with the loss of $-\text{SO}_3$ or $-\text{SO}_3-\text{H}_2\text{O}$, whereas two characteristic fragment ions ($m/z = 302.3054$; 303.3095) were obtained with the loss of $-\text{SO}_3-\text{H}_2\text{O}$. Theoretically, the m/z of fragment ions can increase (+1,+2,+3,+4,+5,+6,+7) corresponding with the number (1,2,3,4,5,6,7) of introduced ^{15}N atoms in PSTs. Based on these data, 2~6 ^{15}N atoms can be introduced into the ^{15}N -PSTs molecule, and 4~6 ^{15}N atoms is most possible.

Table 2. Mass spectral data for gonyautoxins (GTX1-4).

Toxin	Molecular Formula	[M+H] ⁺	Fragment Ion	Loss of	Fragment Ion after Labeling
GTX1	C ₁₀ H ₁₇ N ₇ O ₉ S	412	332; 314	-SO ₃ ; -SO ₃ -H ₂ O	334.3; 318.3; 319.3
GTX4	C ₁₀ H ₁₇ N ₇ O ₉ S	412	332; 314; 253	-SO ₃ ; -SO ₃ -H ₂ O; -SO ₃ -H ₂ O-NH ₃ -CO ₂	318.3; 319.3; 338.3
GTX2	C ₁₀ H ₁₇ N ₇ O ₈ S	396	316; 298	-SO ₃ ; -SO ₃ -H ₂ O;	322.1; 321.1; 305.1
GTX3	C ₁₀ H ₁₇ N ₇ O ₈ S	396	316; 298; 220	-SO ₃ ; -SO ₃ -H ₂ O; -SO ₃ -2H ₂ O-NH ₃ -NHCO	302.3; 303.3

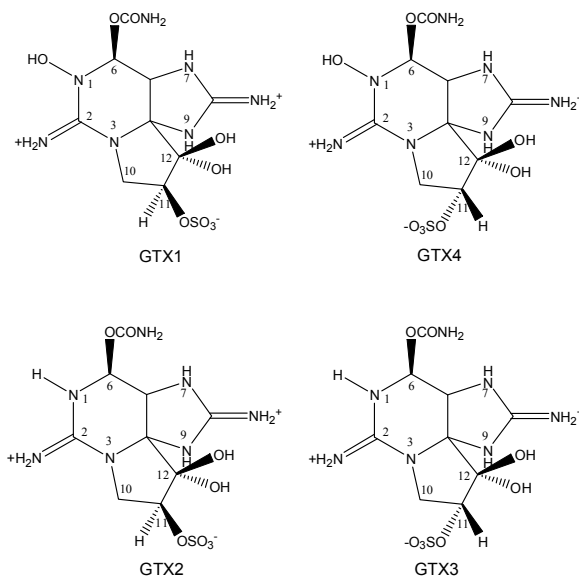


Figure 5. The molecular structural formula of GTX1-4.

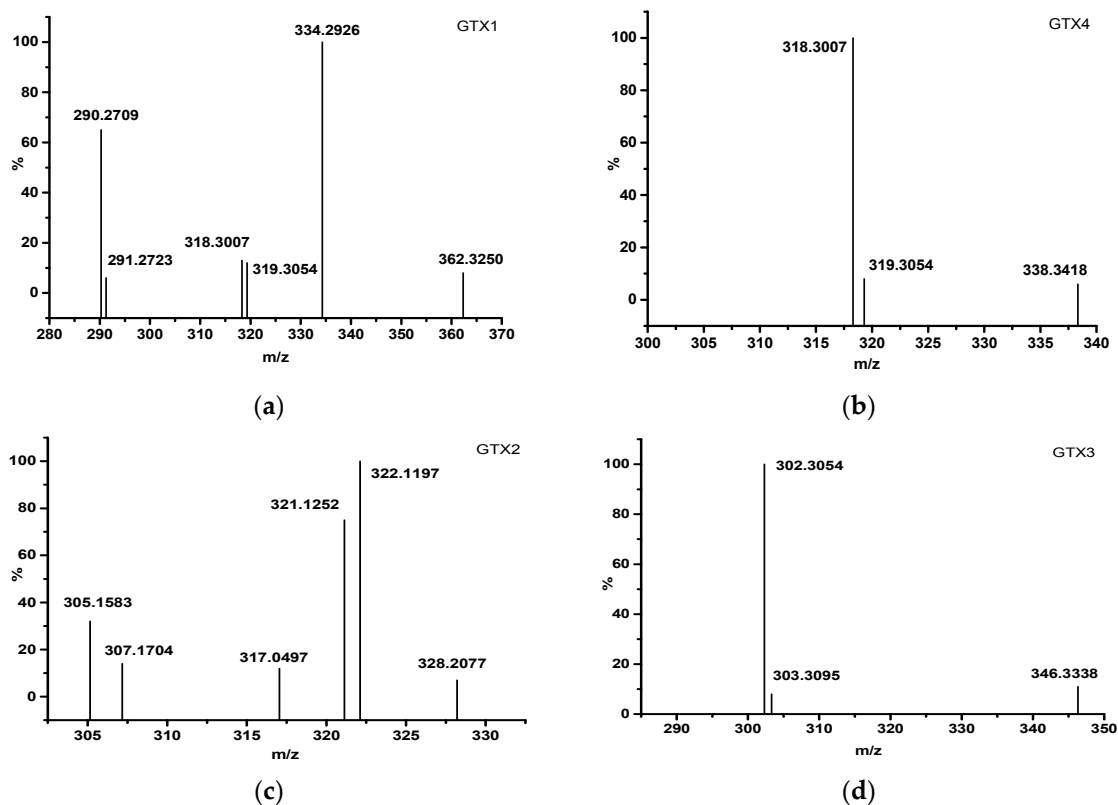


Figure 6. Mass spectrum of ¹⁵N-GTX1 (a), ¹⁵N-GTX4 (b), ¹⁵N-GTX2 (c) and ¹⁵N-GTX3 (d).

3. Discussion

Numerous studies have focused on the bioaccumulation and biotransformation of PSTs using *Alexandrium* strains, such as *A. minutum* in marine organisms [33]. Stable isotopes have been often used to study lipid synthesis, proteomics and ecosystem [13,15,34] and rarely applied to toxin-producing algae [35]. This study intends to use the biosynthetic process to replace the nitrogen atom of *A. minutum* with a stable isotope ^{15}N to form a tracer-enabled *A. minutum* for PST synthesis and metabolism.

3.1. Effect $^{15}\text{N}/\text{P}$ of on *A. minutum* Culture

Growth and toxin production of toxic dinoflagellates vary with nutrients supply. High nutrient cultures can inhibit the photosynthetic capacity of photosystem II, which related to algae growth [27]. The N:P ratio can be used as an index for the nutritional status and physiological behavior of phytoplanktons [36]. Kinds of nitrogen sources and N:P supply ratio can affect the physiological responses of a tropical Pacific strain of *A. minutum*, the cellular toxin quota (Q_t) was higher in P-depleted, nitrate-grown cultures [37]. To assure the feasibility of isotope ^{15}N , some experiments were carried out, including the comparison of different $^{15}\text{N}:\text{P}$ ratio. In batch culture, five $^{15}\text{N}:\text{P}$ ratios were compared, and the growth of *A. minutum* under 1.0 and 1.5 times of the f/2 medium standard $^{15}\text{N}/\text{P}$ concentration was better than others (Figure 1a). Similar previous findings reported that cell densities and growth rates of *A. minutum* were severely suppressed under high N/P ratios (>100) in both N- NO_3 and N- NH_4 treatments [38]. Some studies showed that the incorporation of ^{15}N -labeled salt did not affect the growth of green alga *Chlamydomonas reinhardtii* [24,39], and our study achieved the same result with *A. minutum*. The toxin profile of this *A. minutum* strain is relatively stable and predominantly constitutes GTX1-4 (Figure 3), the same as four strains of *A. minutum* collected from southern Taiwan [40], even under different N:P supply ratios. The highest algae toxicity per cell of all five groups was observed at day 25, and cellular toxin quota of the exponential growth phase was higher than that of the stable phase, even though the total number of stable cells is highest during the entire growth process (Figure 1b). The explanation could be that there was a negative correlation between algae toxicity per cell and cell density. In other words, the cell size was smaller when cell density was higher; thus, toxicity per cell of stable phase was lower. As previously reported, changes of nutrient availability with time in batch culture caused growth stage variability in toxin content, which peaked during mid-exponential growth [31]. Total toxicity, toxicity per cell, and the number of and relative proportion of toxin analogs changed in relation to the $^{15}\text{N}:\text{P}$ ratio. The f/2 medium standard $^{15}\text{N}/\text{P}$ concentration at 1.0 time was a better choice to label PSTs with ^{15}N regardless of cultivation method, i.e., batch culture or generation to generation culture, for *A. minutum* growth, PST production and profile, and experimental cost.

3.2. The Replacement of Stable Isotope ^{15}N

The successful production PSTs of labeled substances from *A. minutum* was detected by MAT-271 Gas isotope mass spectrometer to determine ^{15}N abundance, Analysis by HPLC-MS was performed to identify ^{15}N atom number. In batch culture, $\delta^{15}\text{N}$ of two groups' PSTs had a significant difference ($p < 0.01$) in different growth stages (lag, log, and stable phases) (Table 2). Combining ^{15}N labeling abundance with mass spectrum results, it can be presumed that artificial ^{15}N addition can bring 2~6 ^{15}N atoms into the ^{15}N -PSTs molecule, and the 4~6 ^{15}N atoms' replacement becomes most possible. Recently, ^{15}N stable-isotope-labeling was applied to the toxic dinoflagellate *Alexandrium catenella* and the relationship between the order of ^{15}N incorporation % values of the labeled populations and the proposed biosynthetic route was established [35]. Relative abundance % of m+6 and m+7 isotopomers of PSTs were the highest in *A. catenella* after a two month passage in ^{15}N - NaNO_3 medium in [35], which is similar to our conclusion. Nitrogen (N) isotopic compositions of PSTs in *A. minutum* cells reflect the isotopic fractionations associated with diverse biochemical reactions. Based on PSTs being a secondary metabolite, a small part of the supplied nitrogen was assimilated into PSTs, and most of

the nitrogen may participate in the synthesis of other nitrogen compounds. Some findings on high abundance in biomass (not extracted) have been reported; a process for the cost-effective production of $^{13}\text{C}/^{15}\text{N}$ -labelled biomass of microalgae on a commercial scale is presented, and 97.8% of the supplied nitrogen is assimilated into the biomass [23]. However, in the present paper, ^{15}N -labeling abundance of the ^{15}N -PSTs extract was 82.36%, lower than the abundance of whole cell in existing research [23]. The occurrence of this situation can be explained by the following reasons. Firstly, the time of each generation culture is not sufficiently long enough. Secondly, the total ^{15}N abundance in the crude extract of the toxin cannot fully represent ^{15}N in the pure toxin, because extract impurities (e.g., protein and pigment) can cause interference. Thirdly, trace amounts of nitrogen in natural seawater and the culture solution reagent may affect ^{15}N -labeled PSTs.

4. Conclusions

This paper provides the initial evidence that ^{15}N isotope is feasible to label PSTs in *A. minutum* and worthy of being a powerful tool to conduct PST-related researches. In our study, ^{15}N abundance, PSTs content and profile were detected and the ^{15}N atom number introduced into GTX1-4 should be 4–6. However, it is a pity that the precursor and the biosynthetic intermediates of PSTs in *A. minutum* were not analyzed. Further study is needed to apply isotope-labeling on both toxin-producing algae and vector mollusk species so that we can better elucidate the mechanism of PSTs biosynthesis and metabolism.

5. Materials and Methods

5.1. Chemicals and Analytical Standards

^{15}N - NaNO_3 ($\delta^{15}\text{N} = 99.14\%$) was obtained from SRICI (Shanghai Research Institute of Chemical Industry CO., LTD., Shanghai, China). Bio-gel P-2 (400 mesh), Bio-Rex 70 (400 mesh) were obtained from BIO-RAD (Hercules, CA, USA). Certified reference materials for PSTs, including gonyautoxin 1/4 (GTX 1/4), gonyautoxin 2/3 (GTX 2/3), were purchased from the National Research Council, Institute for Marine Bioscience (Halifax, Canada). Analytical grade solvents were used for extraction purposes while LC grade solvents were used for HPLC-FLD applications.

5.2. Algal Culture

The PSTs-producing dinoflagellate *A. minutum* (strain AGY-H46, purchased from Leadingtec, Shanghai, China) was cultivated in thermo regulated rooms (25 ± 1 °C) with filtered ($0.45 \mu\text{m}$, Jinjing Ltd., China) and sterilized (121 °C, 20 min) seawater before enrichment with f/2 medium amendments (Table 3). The light intensity was set at 3000–4000 lux with a dark:light cycle of 14:10 h. The seawater was obtained from Donghai Island waters (Zhanjiang, China). Algal cell densities were determined by optical microscope and cells were collected at particular time for ^{15}N abundance analysis and PSTs detection.

Table 3. f/2 medium amendments.

	Reagent	Working Solution (mg/L)	Stock Solution (g/L)
A:	NaNO_3	75	75
B:	$\text{NaH}_2\text{PO}_4 \cdot \text{H}_2\text{O}$	5	5
C:	$\text{Na}_2\text{SiO}_3 \cdot 9\text{H}_2\text{O}$	20	20
D:	Na_2EDTA	4.36	4.36
E:	$\text{FeCl}_3 \cdot 6\text{H}_2\text{O}$	3.16	3.16
F:	$\text{CuSO}_4 \cdot 5\text{H}_2\text{O}$	0.01	0.01
	$\text{ZnSO}_4 \cdot 7\text{H}_2\text{O}$	0.023	0.023
	$\text{CoCl}_2 \cdot 6\text{H}_2\text{O}$	0.012	0.012
	$\text{MnCl}_2 \cdot 4\text{H}_2\text{O}$	0.18	0.18
	$\text{Na}_2\text{MoO}_4 \cdot 2\text{H}_2\text{O}$	0.07	0.07

Table 3. Cont.

	Reagent	Working Solution (mg/L)	Stock Solution (g/L)
G:	Vitamin B1	0.1	0.01
	Vitamin B12	0.5×10^{-3}	0.5×10^{-4}
	Vitamin H	0.5×10^{-3}	0.5×10^{-4}

5.3. ^{15}N -PSTs Extraction

An aliquot (60 mL) of the algal fluid was centrifuged at 6000 r/min under 4 °C for 10 min, and the supernatant was carefully discarded. The sedimentary cells were resuspended with 0.05 M acetic acid and then broken using ultrasonic processor in an ice bath for 10 min (power 80%, working 3 s, gap 3 s) until there was no whole cell. The combined liquid was centrifuged at 12000 r/min under 4 °C for 10 min, then the supernatant was filtered (0.22 µm, Jinjing Ltd., China) and stored under −20 °C for purification.

5.4. ^{15}N -PSTs Separation and Purification

Separation and purification were carried on by reference to published papers [41,42]. The PSTs extract was adsorbed to a column of Bio-Gel P-2 equilibrated with water. Furthermore, the column was first washed with a sufficient volume of water and eluted with 0.1 mM acetic acid at a flow rate of 0.5 mL/min. After separation, toxin mixture was purified by ion exchange chromatography using a column of Bio-Rex 70 equilibrated with water and gradient eluted with acetic acid (acetic acid concentration was as follows: 0, 0.05, 0.055 and 0.060 mM). The fraction was collected every 12 min and then analyzed by FFA to assure purification efficiency.

5.5. ^{15}N Abundance Analysis of ^{15}N -PSTs Extracts

^{15}N abundance was analyzed by MAT-271 Gas isotope mass spectrometer (Finnigan, Santa Clara Valley, CA, USA). Operating conditions were set to high voltage (10 kV), emission current (0.040 mA), electronic energy (100 eV) and well voltage (134 eV). ^{15}N -PSTs extraction after freeze-drying was converted to gas by micro-high-heat combustion method, then entered into gas isotope mass spectrometer sample introduction system via sample adapter. Mass spectrometer vacuum was less than 2×10^{-5} Pa. After making the necessary calibration settings for the instrument, the instrument background measurement was performed. The sample gas was introduced into the sample storage system at a pressure of 5–10 Pa. The measurement process was automatically performed by computer instructions, and the signal strength (in mV) of mass number 28, 29, 30 was output as I_{28} , I_{29} and I_{30} .

5.6. PSTs Toxicity Test by the Mouse Bioassay

The mouse bioassay (MBA) was a referenced method from [43]. 10 healthy male mice were injected intraperitoneally with 1 mL aliquot of ^{15}N -PSTs extracts and observed to quantify the toxin according to the time of death. The toxicity was expressed in mouse units (MU), 1 MU representing the average toxin amount to kill a mouse weighing 20 g within 15 min.

5.7. ^{15}N -PSTs Detection by the Fast Fluorimetric Assay (FFA)

The fast fluorimetric assay (FFA) was performed by fluorospectrophotometer (HITACHI, Japan) at a 333 nm excitation wavelength, 10 nm excitation slit, emission wavelength 390 nm and 20 nm emission slit. The method was from [44] and got some modification in this paper. A portion (0.5 mL) of each extract or blank solution (0.05 M acetic acid), respectively, was mixed with 2 mL of oxidation solution (50 mM dipotassium phosphate with 10 mM periodic acid) and incubated for 15 min at 50 °C. After incubation, the reaction mixture was neutralized with 2.5 mL of 1 M acetic acid and transferred to a cuvette for detection by the fast fluorimetric assay (FFA). Relative fluorescence units

(RFU) was recorded and this experiment was conducted to get an overview of the fluorescence of oxidized samples, but not for accurate quantification.

5.8. ^{15}N -PSTs Determination by HPLC-FLD

HPLC-FLD analysis was carried out using Agilent 1100 (Agilent, Santa Clara, CA, USA) coupled to PCX5200 (Pickering Laboratories Company) post-column reactor and Agilent G1321A detector ($\lambda_{\text{ex}} = 330 \text{ nm}$, $\lambda_{\text{em}} = 390 \text{ nm}$). Chromatographic separation of compounds was achieved on a reversed-phase C8 column (150 mm \times 4.6 mm i.d.; 5 μm , GL Sciences, Tokyo, Japan). The system was managed by an Agilent Chem. Station 2.1 workstation. The PST extract was subjected to HPLC-FLD after ultrafiltration (10,000 Da ultrafiltration centrifuge tube, 12,000 r/min for 10 min at 4 $^{\circ}\text{C}$). Analysis method was performed according to [45]. The oxidant solution was 50 mM potassium hydrogen phosphate containing 7 mM periodic acid. The acidifying agent was 0.5 M acetic acid. The flow rates were 0.8 mL/min for the elution solution and 0.4 mL/min for the oxidant and acidifying agent.

5.9. ^{15}N -PSTs Quantification by HPLC-MS

HPLC-MS analysis was carried out on Agilent 1100 (Agilent, USA) coupled to Waters FIN_C2-XS QToF mass spectrometer (Waters, Milford, MA, USA) with an electrospray ionization interface. PSTs were separated on a TSKgel Amide-80 HILIC column (250 mm \times 2 mm i.d.; 5 μm , Tosoh Bioscience, LLC, Montgomeryville, PA, USA). The PSTs extract after purification was subjected to HPLC-MS after ultrafiltration (10000 Da ultrafiltration centrifuge tube, 12000 r/min for 10 min at 4 $^{\circ}\text{C}$). A binary mobile phase included "solvent A" and "solvent B", in which "solvent A" was water containing 2.0 mM ammonium formate containing 0.1% (v/v) formic acid and "solvent B" was acetonitrile containing 0.1% (v/v) formic acid. Parameters of mass spectrometer were multiple reaction monitoring (MRM) mode, positive polarity of ESI, capillary voltage (3.2 kV), ion source temperature (150 $^{\circ}\text{C}$), desolvation temperature (400 $^{\circ}\text{C}$), cone gas flow (50 L/h) and desolvation gas flow (700 L/h).

Author Contributions: Methodology, X.Y.; investigation, M.L., R.Z. and X.H.; writing-original draft preparation, M.L.; writing-review and editing, W.X.; supervision, L.S., and C.L.; project administration, W.X. and X.Y.

Funding: This research was funded by National Natural Science Foundation of China, grant number 31271938 and 31772089, and Shandong Province Key Research and Development Program, grant number 2017GHY15127. This work was also financially supported by Major Scientific Research Projects in Universities Cultivation Plan (Q15137) GDOU2015050202.

Acknowledgments: This research was funded by National Natural Science Foundation of China, grant number 31271938 and 31772089, and Shandong Province Key Research and Development Program, grant number 2017GHY15127. This work was also financially supported by Major Scientific Research Projects in Universities Cultivation Plan (Q15137) GDOU2015050202. We gratefully acknowledge the help of the other members in our lab, who have offered us valuable suggestions in the academic studies. Besides, we also show our gratitude to Shanghai Research Institute of Chemical Industry CO., LTD., which provided technical support for us.

Conflicts of Interest: The authors declare no conflict of interest.

References

1. Hoagland, P.A.; Anderson, D.M.; Kaoru, Y.; White, A.W. The Economic Effects of Harmful Algal Blooms in the United States: Estimates, Assessment Issues, and Information Needs. *Estuaries* **2002**, *25*, 819–837. [[CrossRef](#)]
2. Gustaafm, H. Ocean climate change, phytoplankton community responses, and harmful algal blooms: A formidable predictive challenge. *J. Phycol.* **2010**, *46*, 220–235. [[CrossRef](#)]
3. Rolton, A.; Vignier, J.; Soudant, P.; Shumway, S.E.; Bricelj, V.M.; Volety, A.K. Effects of the red tide dinoflagellate, *Karenia brevis*, on early development of the eastern oyster *Crassostrea virginica* and northern quahog *Mercenaria mercenaria*. *Aquat. Toxicol.* **2014**, *155*, 199–206. [[CrossRef](#)] [[PubMed](#)]
4. Brooks, B.W.; Lazorchak, J.M.; Howard, M.D.; Johnson, M.V.; Morton, S.L.; Perkins, D.A.; Reavie, E.D.; Scott, G.I.; Smith, S.A.; Steevens, J.A. Are harmful algal blooms becoming the greatest inland water quality threat to public health and aquatic ecosystems? *Environ. Toxicol. Chem.* **2016**, *35*, 6–13. [[CrossRef](#)] [[PubMed](#)]

5. Grattan, L.M.; Holobaugh, S.; Morris, J.G. Harmful algal blooms and public health. *Harmful Algae* **2016**, *57*, 2–8. [[CrossRef](#)] [[PubMed](#)]
6. Zhang, Y.; Zhang, S.F.; Lin, L.; Wang, D.Z. Whole Transcriptomic Analysis Provides Insights into Molecular Mechanisms for Toxin Biosynthesis in a Toxic Dinoflagellate *Alexandrium catenella* (ACHK-T). *Toxins* **2017**, *9*, 213. [[CrossRef](#)]
7. Li, A.; Chen, H.; Qiu, J.; Lin, H.; Gu, H. Determination of multiple toxins in whelk and clam samples collected from the Chukchi and Bering seas. *Toxicon* **2016**, *109*, 84–93. [[CrossRef](#)]
8. Jiang, T.; Xu, Y.; Li, Y.; Jiang, T.; Wu, F.; Zhang, F. Seasonal dynamics of *Alexandrium tamarense* and occurrence of paralytic shellfish poisoning toxins in bivalves in Nanji Islands, East China Sea. *Mar. Freshw. Res.* **2014**, *65*, 350. [[CrossRef](#)]
9. Fabioux, C.; Sulistiyani, Y.; Haberkorn, H.; Hegaret, H.; Amzil, Z.; Soudant, P. Exposure to toxic *Alexandrium minutum* activates the detoxifying and antioxidant systems in gills of the oyster *Crassostrea gigas*. *Harmful Algae* **2015**, *48*, 55–62. [[CrossRef](#)]
10. Xie, W.; Liu, X.; Yang, X.; Zhang, C.; Bian, Z. Accumulation and depuration of paralytic shellfish poisoning toxins in the oyster *Ostrea rivularis* Gould—Chitosan facilitates the toxin depuration. *Food Control* **2013**, *30*, 446–452. [[CrossRef](#)]
11. Ding, L.; Qiu, J.; Li, A. Proposed Biotransformation Pathways for New Metabolites of Paralytic Shellfish Toxins Based on Field and Experimental Mussel Samples. *J. Agric. Food Chem.* **2017**, *65*, 5494–5502. [[CrossRef](#)] [[PubMed](#)]
12. Mat, A.M.; Klopp, C.; Payton, L.; Jeziorski, C.; Chalopin, M.; Amzil, Z.; Tran, D.; Wikfors, G.H.; Hegaret, H.; Soudant, P.; et al. Oyster transcriptome response to *Alexandrium* exposure is related to saxitoxin load and characterized by disrupted digestion, energy balance, and calcium and sodium signaling. *Aquat. Toxicol.* **2018**, *199*, 127–137. [[CrossRef](#)] [[PubMed](#)]
13. Han, S.; Yan, S.; Chen, K.; Zhang, Z.; Zed, R.; Zhang, J.; Song, W.; Liu, H. ¹⁵N isotope fractionation in an aquatic food chain: *Bellamyia aeruginosa* (Reeve) as an algal control agent. *J. Environ. Sci.* **2010**, *22*, 242–247. [[CrossRef](#)]
14. Chahrour, O.; Cobice, D.; Malone, J. Stable isotope labelling methods in mass spectrometry-based quantitative proteomics. *J. Pharm. Biomed. Anal.* **2015**, *113*, 2–20. [[CrossRef](#)] [[PubMed](#)]
15. Brandsma, J.; Bailey, A.P.; Koster, G.; Gould, A.P.; Postle, A.D. Stable isotope analysis of dynamic lipidomics. *Biochim. Biophys. Acta* **2017**, *1862*, 792–796. [[CrossRef](#)]
16. Schneider, L.; Maher, W.A.; Potts, J.; Taylor, A.M.; Batley, G.E.; Krikowa, F.; Adamack, A.; Chariton, A.A.; Gruber, B. Trophic transfer of metals in a seagrass food web: Bioaccumulation of essential and non-essential metals. *Mar. Pollut. Bull.* **2018**, *131*, 468. [[CrossRef](#)] [[PubMed](#)]
17. He, Y.-L.; Luo, Y.-B.; Chen, H.; Hou, H.-W.; Hu, Q.-Y. Research Progress in Analysis of Small Molecule Metabolites in Bio-matrices by Stable Isotope Coded Derivatization Combining with Liquid Chromatography–tandem Mass Spectrometry. *Chin. J. Anal. Chem.* **2017**, *45*, 1066–1077. [[CrossRef](#)]
18. Thomas, M.; Huck, N.; Hoehenwarter, W.; Conrath, U.; Beckers, G.J.M. *Combining Metabolic ¹⁵N Labeling with Improved Tandem MOAC for Enhance*; Springer: New York, NY, USA, 2015; pp. 81–96.
19. Lehmann, W.D. A timeline of stable isotopes and mass spectrometry in the life sciences. *Mass Spectrom. Rev.* **2016**, *36*. [[CrossRef](#)]
20. Bequette, B.J.; Backwell, F.R.C.; Calder, A.G.; Metcalf, J.A.; Beever, D.E.; Macrae, J.C.; Loble, G.E. Application of a U-¹³C-Labeled Amino Acid Tracer in Lactating Dairy Goats for Simultaneous Measurements of the Flux of Amino Acids in Plasma and the Partition of Amino Acids to the Mammary Gland. *J. Dairy Sci.* **1997**, *80*, 2842–2853. [[CrossRef](#)]
21. Cox, J.; Kyle, D.; Radmer, R.; Delente, J. Stable-isotope-labeled biochemicals from microalgae. *Trends Biotechnol.* **1988**, *6*, 279–282. [[CrossRef](#)]
22. Fernández, F.G.A.; Alias, C.B.; Pérez, J.A.S.; Sevilla, J.M.F.; González, M.J.I.; Grima, E.M. Production of ¹³C polyunsaturated fatty acids from the microalga *Phaeodactylum tricorutum*. *J. Appl. Phycol.* **2003**, *15*, 229–237. [[CrossRef](#)]
23. Acien Fernandez, F.G.; Fernandez Sevilla, J.M.; Egorova-Zachernyuk, T.A.; Molina Grima, E. Cost-effective production of ¹³C, ¹⁵N stable isotope-labelled biomass from phototrophic microalgae for various biotechnological applications. *Biomol. Eng.* **2005**, *22*, 193–200. [[CrossRef](#)] [[PubMed](#)]

24. Carcelén, J.N.; Marchante-Gayón, J.M.; González, P.R.; Valledor, L.; Cañal, M.J.; Alonso, J.I.G. A cost-effective approach to produce ¹⁵N-labelled amino acids employing *Chlamydomonas reinhardtii* CC503. *Microb. Cell Factories* **2017**, *16*, 146. [[CrossRef](#)] [[PubMed](#)]
25. Wiese, M.; D'Agostino, P.M.; Mihali, T.K.; Moffitt, M.C.; Neilan, B.A. Neurotoxic alkaloids: Saxitoxin and its analogs. *Mar. Drugs* **2010**, *8*, 2185–2211. [[CrossRef](#)] [[PubMed](#)]
26. Hwang, D.F.; Lu, Y.H. Influence of environmental and nutritional factors on growth, toxicity, and toxin profile of dinoflagellate *Alexandrium minutum*. *Toxicon* **2000**, *38*, 1491–1503. [[CrossRef](#)]
27. Hui, G.; Jianting, Y.; Zhongmin, S.; Delin, D. Effects of salinity and nutrients on the growth and chlorophyll fluorescence of *Caulerpa lentillifera*. *Chin. J. Oceanol. Limnol.* **2015**, *33*, 410–418. [[CrossRef](#)]
28. Boyer, G.L.; Sullivan, J.J.; Andersen, R.J.; Harrison, P.J.; Taylor, F.J.R. Effects of nutrient limitation on toxin production and composition in the marine dinoflagellate *Protogonyaulax tamarensis*. *Mar. Boil.* **1987**, *96*, 123–128. [[CrossRef](#)]
29. Hamasaki, K.; Horie, M.; Tokimitsu, S.; Toda, T.; Taguchi, S. Variability in Toxicity of the Dinoflagellate *Alexandrium Tamarensis* Isolated from Hiroshima Bay, Western Japan, as a Reflection of Changing Environmental Conditions. *J. Plankton Res.* **2001**, *23*, 271–278. [[CrossRef](#)]
30. Wang, D.-Z.; Hsieh, D.P.H. Growth and toxin production in batch cultures of a marine dinoflagellate *Alexandrium tamarensis* HK9301 isolated from the South China Sea. *Harmful Algae* **2005**, *4*, 401–410. [[CrossRef](#)]
31. Anderson, D.M.; Kulis, D.M.; Sullivan, J.J.; Hall, S.; Lee, C. Dynamics and physiology of saxitoxin production by the dinoflagellates *Alexandrium* spp. *Mar. Boil.* **1990**, *104*, 511–524. [[CrossRef](#)]
32. Dell'Aversano, C.; Hess, P.; Quilliam, M.A. Hydrophilic interaction liquid chromatography–mass spectrometry for the analysis of paralytic shellfish poisoning (PSP) toxins. *J. Chromatogr. A* **2005**, *1081*, 190–201. [[CrossRef](#)] [[PubMed](#)]
33. Guéguen, M.; Baron, R.; Bardouil, M.; Truquet, P.; Haberkorn, H.; Lassus, P.; Barillé, L.; Amzil, Z. Modelling of paralytic shellfish toxin biotransformations in the course of *Crassostrea gigas* detoxification kinetics. *Ecol. Model.* **2011**, *222*, 3394–3402. [[CrossRef](#)]
34. Brandsma, J.; Postle, A.D. Analysis of the regulation of surfactant phosphatidylcholine metabolism using stable isotopes. *Ann. Anat. Anat. Anz.* **2017**, *211*, 176–183. [[CrossRef](#)] [[PubMed](#)]
35. Cho, Y.; Tsuchiya, S.; Omura, T.; Koike, K.; Oikawa, H.; Konoki, K.; Oshima, Y.; Yotsu-Yamashita, M. Metabolomic study of saxitoxin analogues and biosynthetic intermediates in dinoflagellates using (15)N-labelled sodium nitrate as a nitrogen source. *Sci. Rep.* **2019**, *9*, 3460. [[CrossRef](#)] [[PubMed](#)]
36. Roelke, D.L.; Eldridge, P.M.; Cifuentes, L.A. A Model of Phytoplankton Competition for Limiting and Nonlimiting Nutrients: Implications for Development of Estuarine and Nearshore Management Schemes. *Estuaries* **1999**, *22*, 92–104. [[CrossRef](#)]
37. Hii, K.S.; Lim, P.T.; Kon, N.F.; Takata, Y.; Usup, G.; Leaw, C.P. Physiological and transcriptional responses to inorganic nutrition in a tropical Pacific strain of *Alexandrium minutum*: Implications for the saxitoxin genes and toxin production. *Harmful Algae* **2016**, *56*, 9–21. [[CrossRef](#)] [[PubMed](#)]
38. Lim, P.T.; Leaw, C.P.; Kobiyama, A.; Ogata, T. Growth and toxin production of tropical *Alexandrium minutum* Halim (Dinophyceae) under various nitrogen to phosphorus ratios. *J. Appl. Phycol.* **2010**, *22*, 203–210. [[CrossRef](#)]
39. Sauer, M.L.A.; Xu, B.; Sutton, F. Metabolic labeling with stable isotope nitrogen (¹⁵ N) to follow amino acid and protein turnover of three plastid proteins in *Chlamydomonas reinhardtii*. *Proteome Sci.* **2014**, *12*, 1–9. [[CrossRef](#)]
40. Chou, H.N.; Chen, Y.M.; Chen, C.Y. Variety of PSP toxins in four culture strains of *Alexandrium minutum* collected from southern Taiwan. *Toxicon* **2004**, *43*, 337–340. [[CrossRef](#)]
41. Miao, Y.P.; Zhou, H.N.; Wen, R. Isolation and purification of gonyautoxins from *Alexandrium minutum* Halim. *Acta Pharm. Sin.* **2004**, *39*, 52–55. [[CrossRef](#)]
42. Laycock, M.V.; Thibault, P.; Ayer, S.W.; Walter, J.A. Isolation and purification procedures for the preparation of paralytic shellfish poisoning toxin standards. *Neurogastroenterol. Motil.* **2010**, *2*, 175–183. [[CrossRef](#)]
43. AOAC. AOAC Official Method 959.08: Paralytic Shellfish Poison, Biological Method; AOAC: Arlington, VA, USA, 2000.

44. Gerdtts, G.; Hummert, C.; Donner, G.; Luckas, B.; Schütt, C. A fast fluorimetric assay (FFA) for the detection of saxitoxin in natural phytoplankton samples. *Mar. Ecol. Prog.* **2002**, *230*, 29–34. [[CrossRef](#)]
45. Van De Riet, J.; Gibbs, R.S.; Muggah, P.M.; Rourke, W.A.; Macneil, J.D.; Quilliam, M.A. Liquid chromatography post-column oxidation (PCOX) method for the determination of paralytic shellfish toxins in mussels, clams, oysters, and scallops: Collaborative study. *J. AOAC Int.* **2011**, *94*, 1154–1176. [[PubMed](#)]



© 2019 by the authors. Licensee MDPI, Basel, Switzerland. This article is an open access article distributed under the terms and conditions of the Creative Commons Attribution (CC BY) license (<http://creativecommons.org/licenses/by/4.0/>).